



Synthesis, characterization and electrocatalytic activity for ethanol oxidation of carbon supported Pt, Pt–Rh, Pt–SnO₂ and Pt–Rh–SnO₂ nanoclusters

A. Kowal^{a,b,*}, S.Lj. Gojković^c, K.-S. Lee^d, P. Olszewski^a, Y.-E. Sung^d

^a Institute of Catalysis and Surface Chemistry, Polish Academy of Sciences, ul. Niezapominajek 8, 30-239 Krakow, Poland

^b Institute of Non-Ferrous Metals Department in Poznan, Central Laboratory of Batteries and Cells, Poznan, Poland

^c Faculty of Technology and Metallurgy, University of Belgrade, Belgrade, Serbia

^d School of Chemical and Biological Engineering and Research Center for Energy Conversion and Storage, Seoul National University, Seoul, South Korea

ARTICLE INFO

Article history:

Received 15 October 2008

Received in revised form 19 January 2009

Accepted 19 January 2009

Available online 24 January 2009

Keywords:

Pt–Rh–SnO₂ nanocatalyst

Ethanol electrooxidation

Direct ethanol fuel cell

Polyol synthesis

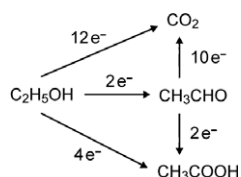
ABSTRACT

Nanoclusters of Pt, Pt–Rh, Pt–SnO₂ and Pt–Rh–SnO₂ were successfully synthesized by polyol method and deposited on high-area carbon. HRTEM and XRD analysis revealed two phases in the ternary Pt–Rh–SnO₂/C catalyst: solid solution of Rh in Pt and SnO₂. The activity of Pt–Rh–SnO₂/C for ethanol oxidation was found to be much higher than Pt/C and Pt–Rh/C and also superior to Pt–SnO₂/C. Quasi steady-state measurements at various temperatures (30–60 °C), ethanol concentrations (0.01–1 M) and H₂SO₄ concentrations (0.02–0.5 M) showed that Pt–Rh–SnO₂/C is about 20 times more active than Pt/C in the potential range of interest for the fuel cell application.

© 2009 Elsevier B.V. All rights reserved.

1. Introduction

Direct alcohol fuel cell working with ethanol has received growing attention because ethanol is low-toxic and renewable biofuel which can be produced from fermentation of biomass [1,2]. Its complete oxidation to CO₂ yields 12 electrons per molecule, but the reaction on Pt is slow and the main product is not CO₂ but acetaldehyde and acetic acid [3,4]. The possible reaction paths of ethanol oxidation reaction (EOR) can be represented as [4]:



When Ru or Sn are added to Pt, EOR starts at less positive potentials and the current densities are higher, but selectivity towards CO₂ is even lower [5]. The catalyst composed of Pt and SnO_x nanoclusters showed slightly higher selectivity compared to Pt–Sn alloys, but main product is still acetaldehyde and selectivity towards CO₂ is even lower than on Pt [5–7]. However, Rh can increase CO₂ yield

by facilitating C–C bond cleavage. This effect was reported firstly for the electrodeposited Pt–Rh layers [8] and recently proved for Pt–Rh/C catalysts [9]. Unfortunately, current densities for EOR on both catalysts were not increased by the addition of Rh. It was proposed that the strong CO–Rh bond or slow dehydrogenation on Rh diminish overall EOR rate.

Comparing the influences of Ru or Sn/SnO_x and Rh, one can assume that only a ternary catalyst can provide both high activity and high selectivity. Pt–Ru–Rh/C showed to be a compromise between overall reaction rate and CO₂ yield, i.e. both characteristics were between those of Pt–Ru/C and Pt–Rh/C [10]. Ternary Pt–Sn–Rh/C catalyst was also tested, but in the low potential region its activity was lower than that of binary Pt–Sn/C catalyst [11]. However, Pt supported on Sb-doped SnO₂ exhibited much higher activity for EOR and thermal stability than Pt/C [12]. Recently nanoclusters of Pt–Rh–SnO₂ supported on high-area carbon were synthesized by cation-adsorption/reduction-galvanic-displacement method [13] and showed to be very effective in C–C bond splitting in ethanol, causing its predominant oxidation to CO₂. In this paper, we show the performance of the Pt–Rh–SnO₂ catalyst synthesized by polyol method and compare it to the Pt and the binary catalysts.

2. Experimental

2.1. Preparation of the catalysts

Stable Pt, Pt–Rh and SnO₂ nanoclusters were prepared by polyol method [14,15] in the absence of any capping agents. In brief,

* Corresponding author. Address: Institute of Catalysis and Surface Chemistry, Polish Academy of Sciences, ul. Niezapominajek 8, 30-239 Krakow, Poland.
E-mail address: nckowal@cyf-kr.edu.pl (A. Kowal).

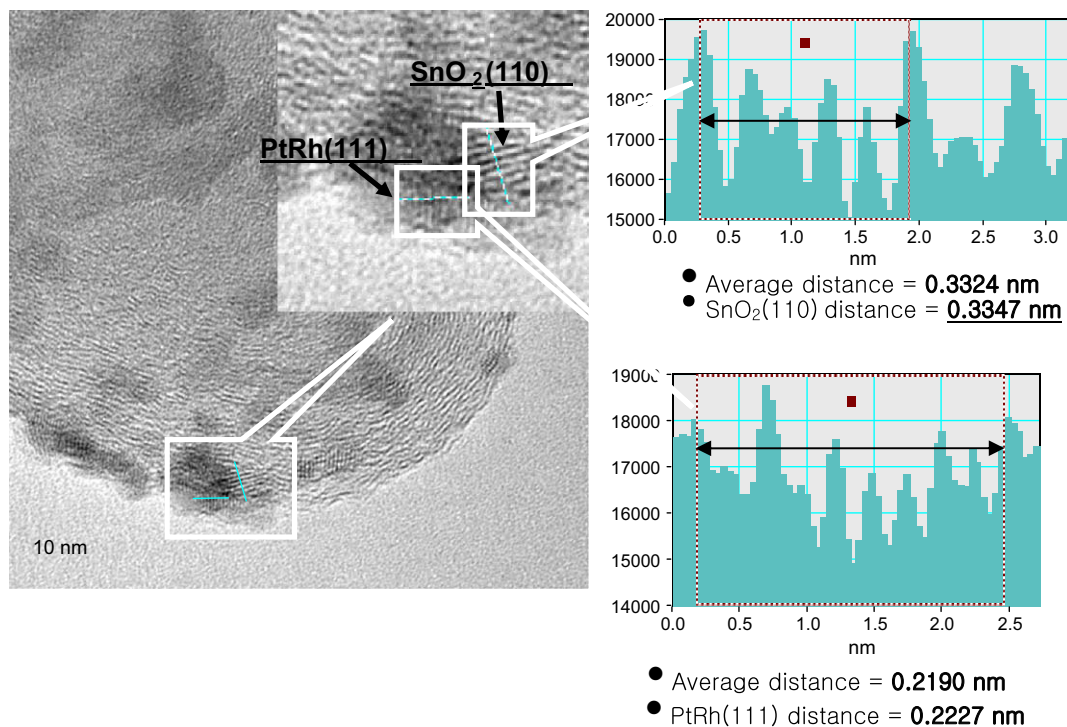


Fig. 1. TEM and HRTEM images of Pt–Rh–SnO₂/C and the pixel intensity profiles for SnO₂ and Pt–Rh crystallites.

H₂PtCl₆ · xH₂O, RhCl₃ · xH₂O and SnO₂ were dissolved in water, then ethylene-glycol (EG) and NaOH were added (only EG in the case of SnO₂) and a solution of single precursor or a mixture of precursor solutions were refluxed in Ar flow. Afterward a colloid solution was mixed with high-area carbon (Vulcan XC-72), water and H₂SO₄ and stirred for 3 h. After filtering and drying, the powder was heated in Ar flow at 160 °C. In all cases, the amount of colloid and carbon was adjusted to the loading of 20 mass% of the catalyst.

2.2. TEM and XRD characterization of the catalysts

Catalyst nanoparticles deposited on high-area carbon were examined by transmission electron microscopy (TEM) using JEOL 2010 operated at 200 kV. The X-ray diffraction (XRD) measurement was performed with a D5005 diffractometer (Bruker-AXS, Germany)

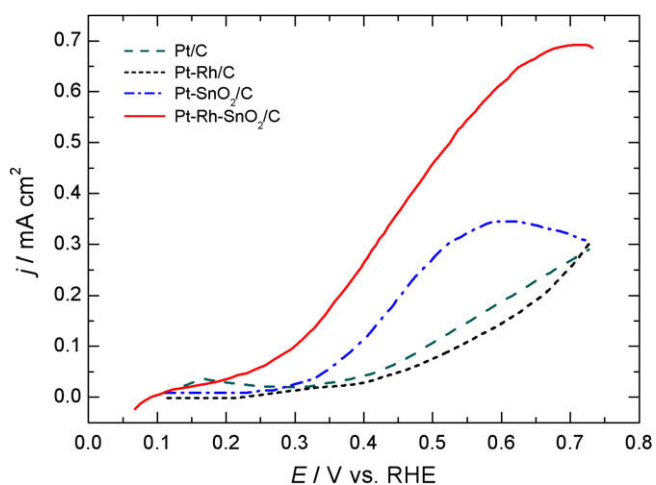


Fig. 2. Potentiodynamic polarization curves of EOR recorded in 0.5 M H₂SO₄ + 1 M C₂H₅OH solution. Scan rate 50 mV s⁻¹, temperature 20 °C.

equipped with CuKα source. Data were collected with 0.05°/2 s step size. Quantitative analysis was carried out with Rietveld refinement using TOPAS software.

2.3. Electrochemical measurements

The catalyst powders were suspended in water and Nafion solution and applied onto a glassy-carbon electrode [16]. A standard cell with a Pt counter electrode and a saturated calomel reference electrode was used. The electrolyte contained H₂SO₄ and C₂H₅OH. It was prepared with high purity water and deaerated by N₂.

After having immersed the electrode in the supporting electrolyte, the potential was cycled between 0 and 1.2 V (RHE) in the case of Pt/C catalyst and between 0 and 0.8 V (RHE) in the case of other catalysts in order to prevent dissolution of Rh and Sn. Upon a steady-state voltammogram was achieved, in the positive going sweep the potential was held at 0.1 V (RHE), C₂H₅OH was added into the electrolyte and after 2 min, the sweep was continued at 50 mV s⁻¹ (potentiodynamic test) or at 1 mV s⁻¹ (quasi steady-state polarization measurements).

The currents of EOR were normalized to the Pt surface area in the catalyst which was determined after Rh and Sn were leached from the catalyst surface by the potential cycling between 0 and 1.3 V (RHE) until Pt-like voltammogram was attained. No significant roughening of the Pt surface after the potential cycling was observed. From such a voltammogram H_{upd} desorption charge was estimated and divided by 210 μC cm⁻² corresponding to the hydrogen monolayer.

3. Results and discussion

3.1. Characterization of the Pt–Rh–SnO₂/C powder

All the catalysts were examined by TEM imaging. Fig. 1 shows an image of Pt–Rh–SnO₂/C. In the high magnification image of a cluster of two metallic phases, their lattices can be observed in the

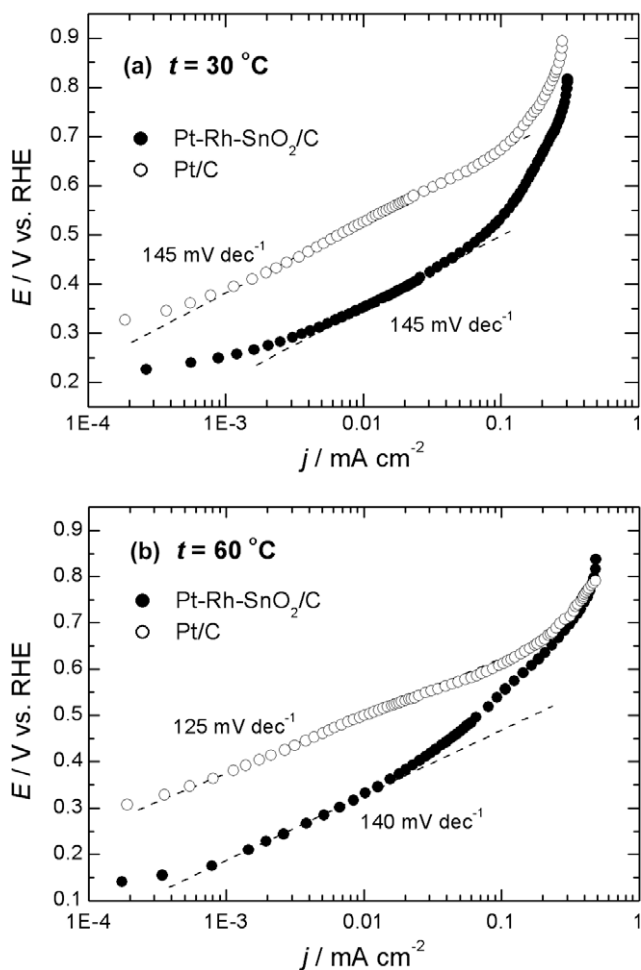


Fig. 3. Tafel plots for EOR recorded in 0.5 M H₂SO₄ + 0.5 M C₂H₅OH solution at (a) 30 °C and (b) 60 °C. Scan rate 1 mV s⁻¹.

bright field due to the phase contrast. Pixel intensity profile of the brighter cluster reveals that the distance between the adjacent fringes is 0.3324 nm, which corresponds to the interplanar distance of the tetragonal SnO₂ (110), $d_{110} = 0.3353$ nm. For the darker colored cluster, the pixel intensity profile indicates the average distance between the adjacent fringes of 0.2190 nm, which is close to the interplanar distance of fcc Pt–Rh (111), $d_{111} = 0.2227$ nm. Particle size analysis shows that the diameters of Pt–Rh and SnO₂ clusters are in the range 1–3 and 3–5 nm, respectively.

The XRD analysis of Pt–Rh–SnO₂/C catalyst confirmed presence of two phases: tetragonal SnO₂ and cubic phase of Pt–Rh solid solution. The composition was found to be 28 mol% of Pt–Rh and 72 mol% of SnO₂, what is close to the nominal 33 mol% of Pt–Rh and 66 mol% SnO₂.

3.2. Potentiodynamic polarization test of the activity of the catalysts

Fast screening of the activity toward EOR of all the catalysts synthesized was carried out by potentiodynamic polarization in 0.5 M H₂SO₄ containing 1 M C₂H₅OH. Fig. 2 shows that the curves for Pt/C and Pt–Rh/C practically overlap, which is in accord with the results of Lima and Gonzales [10]. Fraction of C₂H₅OH molecules with split C–C bond should be higher in the presence of Rh [8,9], but due to sluggish oxidation of CO_{ads} to CO₂, the reaction path via acetaldehyde is likely to be diminished. Thus, in Pt–Rh/C catalyst the positive and the negative effects of Rh cancel.

As data in Fig. 2 evidence, the addition of SnO₂ to Pt improves the EOR kinetics. The onset potential for EOR on Pt/SnO₂/C is

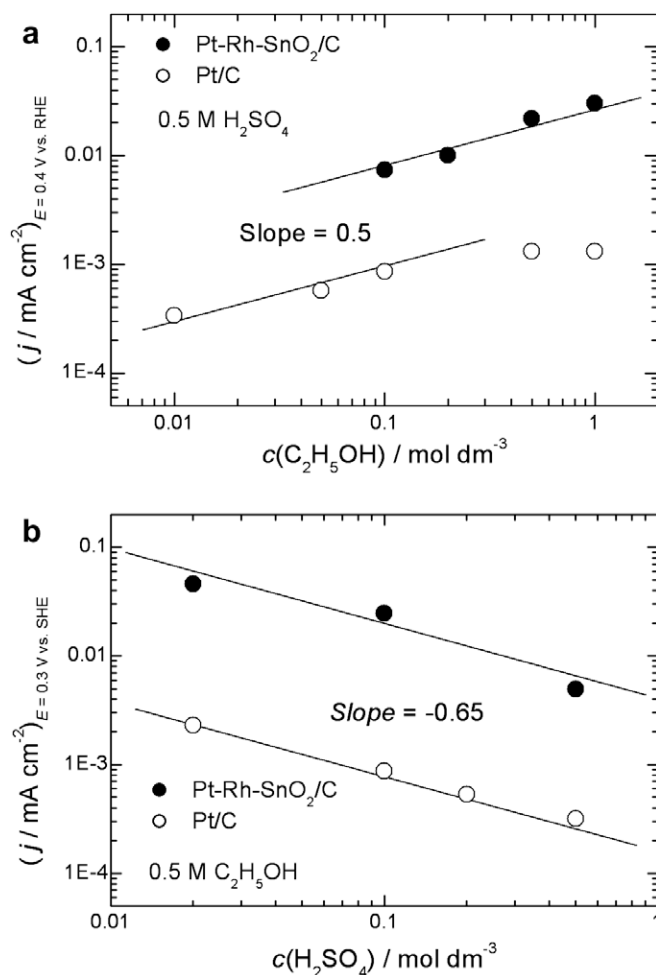


Fig. 4. Dependence of EOR on (a) C₂H₅OH concentration and (b) H₂SO₄ concentration. Data taken from the polarization curves recorded at 30 °C at 1 mV s⁻¹.

~100 mV less positive than on Pt/C and current densities are higher in the whole potential range, confirming the beneficial effect of Sn to EOR on Pt [5]. However, the activity of ternary catalyst, i.e. Pt–Rh/SnO₂/C is higher than that of Pt–SnO₂/C, despite the fact that addition of Rh to Pt has no effect on the reaction rate. Therefore, the Pt–Rh–SnO₂/C catalyst exhibited the best performance and we examined in detail EOR kinetics on this material under the quasi steady-state conditions and compared it with Pt/C.

3.3. Quasi steady-state polarization curves

Polarization curves for EOR on Pt–Rh–SnO₂/C and Pt/C were recorded by slow sweep of 1 mV s⁻¹ in 0.5 M H₂SO₄ containing 0.5 M C₂H₅OH at 30 and 60 °C. These results are given in Fig. 3 in the form of Tafel plots. Both sets of data show that the reaction commences earlier on Pt–Rh–SnO₂/C and that the current densities on this catalyst are higher by more than one order of magnitude in the potential range of interest for the fuel cell applications. In order to see whether such a pronounced difference in the activity remains in the electrolytes of various compositions, the dependence of EOR on H⁺ and ethanol concentration was examined.

Polarization curves were recorded in 0.5 M H₂SO₄ containing 0.01–1 M C₂H₅OH and in 0.02–0.5 M H₂SO₄ containing 0.5 M C₂H₅OH. The current densities at constant potential are plotted as a function of ethanol concentration (Fig. 4a) and as a function of H⁺ concentration (Fig. 4b). EOR on Pt–Rh–SnO₂/C and Pt/C shows the same dependence on H⁺ concentration with the reaction order

with respect to H^+ of -0.65 . Regarding the influence of the ethanol concentration, independence of the reaction rate on Pt/C at high concentration indicates high coverage by the adsorbed residues of ethanol molecules. On Pt–Rh– SnO_2 /C the reaction rate increases with the increase of ethanol concentration with the slope of 0.5 also at high concentrations. This is probably due to facilitated oxidative removal of the ethanol residues, as already shown for the same type of the catalyst [13].

4. Conclusions

Ternary catalyst Pt–Rh– SnO_2 supported on high-area carbon was successfully synthesized by polyol method. HRTEM and XRD analysis revealed two phases: solid solution of Rh in Pt and SnO_2 . The activity of Pt–Rh– SnO_2 /C for EOR was found to be higher than that of Pt/C, Pt–Rh/C and Pt– SnO_2 /C. It was proven that three-functional catalyst is necessary for efficient EOR: Pt for adsorption of C_2H_5OH molecule, Rh for facilitating of C–C bond splitting and SnO_2 for the oxidative removal of CO_{ads} produced due to C–C bond splitting. Further increase in the catalyst activity can be achieved by tuning Pt:Rh: SnO_2 ratio and by increasing the number of twinned Pt–Rh and SnO_2 crystallites. In the case of the catalyst synthesized by cation-adsorption/reduction-galvanic-displacement method [13], where Pt and Rh were deposited right on SnO_2 nanoclusters, higher activity for EOR was demonstrated, because

C_2H_5OH molecule has to be in contact with all phases of the catalyst in order to be completely oxidized.

References

- [1] S. Song, P. Tsiakaras, *Appl. Catal. B: Environ.* 63 (2006) 187–193.
- [2] E. Antolini, *J. Power Sources* 170 (2007) 1.
- [3] H. Wang, Z. Jusys, R.J. Behm, *J. Phys. Chem. B* 108 (2004) 19413.
- [4] G.A. Camara, T. Iwasita, *J. Electroanal. Chem.* 578 (2005) 315.
- [5] Q. Wang, G.Q. Sun, L.H. Jiang, Q. Xin, S.G. Sun, Y.X. Jiang, S.P. Chen, Z. Jusys, R.J. Behm, *Phys. Chem. Chem. Phys.* 9 (2007) 2686.
- [6] F.C. Simões, D.M. dos Anjos, F. Vigier, J.M. Léger, F. Hahn, C. Coutanceau, E.R. Gonzalez, G. Tremiliosi-Filho, A.R. de Andrade, P. Olivi, K.B. Kokoh, *J. Power Sources* 167 (2007) 1.
- [7] S. Rousseau, C. Coutanceau, C. Lamy, J.-M. Léger, *J. Power Sources* 158 (2006) 18–24.
- [8] J.P.I. de Souza, S.L. Queiroz, K. Bergamaski, E.R. Gonzales, F.C. Nart, *J. Phys. Chem. B* 106 (2002) 9825.
- [9] K. Bergamaski, E.R. Gonzales, F.C. Nart, *Electrochim. Acta* 53 (2008) 4396.
- [10] F.H.B. Lima, E.R. Gonzales, *Electrochim. Acta* 53 (2008) 2963.
- [11] F. Colmati, E. Antolini, E.R. Gonzales, *J. Alloy Compd.* 456 (2008) 264.
- [12] K.-S. Lee, I.-S. Park, Y.-H. Cho, D.-S. Jung, N. Jung, H.-Y. Park, Y.-E. Sung, *J. Catal.* 258 (2008) 143.
- [13] A. Kowal, M. Li, M. Shao, K. Sasaki, M.B. Vukmirovic, J. Zhang, N.S. Marinkovic, P. Liu, A.I. Frenkel, R.R. Adzic, *Nat. Mater.*, in press (doi: 10.1038/NMAT 2359).
- [14] Y. Wang, J. Zhang, X. Wang, J. Ren, B. Zuo, Y. Tang, *Top. Catal.* 35 (2005) 35.
- [15] L. Jiang, G. Sun, Z. Zhou, S. Sun, Q. Wang, S. Yan, H. Li, J. Tian, J. Guo, B. Zhou, Q. Xin, *J. Phys. Chem. B* 109 (2005) 8774.
- [16] S.Lj. Gojković, A.V. Tripković, R.M. Stevanović, *J. Serb. Chem. Soc.* 72 (2007) 1419.